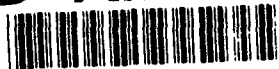


AD-A272 101



2

OFFICE OF NAVAL RESEARCH

Grant N00014-90-I-1971

R&T Code 4131pc1

Technical Report No. 10

Rotational Spectrum of a Dark State in 2-Fluoroethanol Using
Microwave/Radiofrequency-Infrared Multiple Resonance

by

C.C. Miller and L. A. Philips

Cornell University
Department of Chemistry
Ithaca, NY 14853-1301

and

A.M. Andrews, G.T. Fraser, B.H. Pate, and R.D. Suenram

Molecular Physics Division
National Institute of Standards and Technology
Gaithersburg, MD 20899

Prepared for Publication
in the
Journal of Chemical Physics

October 26, 1993

S DTIC
ELECTE
NOV 05 1993
A **D**

Reproduction in whole or in part is permitted for any purpose of the United States Government

This document has been approved for public release and sale; its distribution is unlimited.

93-26701



32P8

80 11 8 040

Rotational Spectrum of a Dark State in 2-Fluoroethanol
Using Microwave/Radiofrequency-Infrared Multiple Resonance

C.C. Miller and L.A. Philips

Department of Chemistry

Cornell University

Ithaca, NY 14853

and

A.M. Andrews, G.T. Fraser, B.H. Pate, and R.D. Suenram

Molecular Physics Division

National Institute of Standards and Technology

Gaithersburg, MD 20899

Abstract

Microwave/radiofrequency-infrared multiple resonance has been used with an electric-resonance optothermal spectrometer to characterize a weak 21.6 MHz perturbation in the infrared spectrum of the ν_{14} C-O stretching vibration of 2-fluoroethanol. The infrared spectrum of 2-fluoroethanol was recorded at a resolution of ~ 2 MHz using a tunable microwave-sideband CO₂ laser. The spectrum is fit by an asymmetric-rotor Hamiltonian to a precision of 0.6 MHz, except for the transitions to the 4_{13} upper state which are split into doublets by an interaction between the 4_{13} level and a rotational level of a nearby background, or dark, vibrational state. Microwave/radiofrequency-infrared double and triple resonance reveals that the 4_{13} level of the C-O stretching vibration is interacting with the 4_{31} level of the dark state. The rotational

Availability Codes	
Dist	Avail and/or Special
A-1	

constants determined for the dark state allow us to assign the perturbing state to the $\nu_{18}+4\nu_{21}$ combination vibration of the lowest energy conformer, where ν_{18} is the CCO bending vibration and ν_{21} is the C-C torsional vibration. From the weak $\Delta K_0 = 2$ matrix element between ν_{14} and $\nu_{18}+4\nu_{21}$ it is possible to derive a $J = 0$ anharmonic interaction between these states of ~ 3.5 GHz.

Introduction

The study of the vibrational dynamics of molecules by high-resolution spectroscopy falls into one of two regimes. In regions of low total vibrational state density the vibrational couplings involve only a few states. In this regime traditional spectroscopic techniques are used to deperturb and assign vibrational state labels. In addition, determination of the coupling strengths between vibrational modes provide detailed mechanistic information about the dynamics.

In the limit of large vibrational state density, the spectrum is too complicated to deperturb. Therefore, phenomenological models [1-3] are used to obtain dynamical information. In the high-density-of-states regime (> 100 states/cm⁻¹) the spectrum is interpreted in terms of intramolecular vibrational energy redistribution (IVR). Spectral analysis provides the time scale of energy localization in the initially excited vibration.

One common feature of spectra in regions of modest state density (< 10 states/cm⁻¹) is the appearance of isolated perturbations which appear at only a few sequential rotational

angular momentum (J) states and are usually weak in magnitude. The rapid tuning in and out of resonance of these interactions often results in a single perturbed rotational state, making it difficult to determine the identity of the perturbing state or the coupling matrix element responsible for the interaction. These weak perturbations are typically neglected in the analysis of infrared spectra since the single-photon absorption spectrum provides little information about these interactions. Here, we show that microwave-infrared multiple-resonance spectroscopy can be used to perform rotational spectroscopy in the perturbing state, thereby providing rotational assignments and spectroscopic constants for the dark state. An understanding of the very near-resonant weak interactions at low energies is important for interpreting spectra at higher energies where the total vibrational state density often results in numerous couplings.

Here, we report the analysis of the ν_{14} C-O stretching fundamental vibration of 2-fluoroethanol near 1089 cm^{-1} . We have studied a number of molecules in the $900 - 1800\text{ cm}^{-1}$ region and find that the presence of isolated perturbations is frequent even at these low energies. Working in regions of low state density makes deperturbation easier for two reasons. First, when the state density is low, it is typically possible to treat the perturbation using a 2×2 interaction matrix. Also, with these isolated resonance interaction with a third resonance state is unlikely. Thus, the rotational constants of the perturbing state are not significantly contaminated by an interaction with a third

state. Second, there are fewer vibrational states that are candidates for the assignment of the dark state. Moreover, most of these states involve combinations of only a few quanta of lower frequency vibrations, reducing the uncertainties in the energy positions of the states.

Interest in 2-fluoroethanol stems from the presence of two large amplitude motions in the molecule: the torsion about the C-C bond and the torsion about the C-O bond. These two coordinates lead to the possibility of five noneclipsed molecular conformations, each having distinct rotational constants. The microwave measurements of Buckton and Azrak [4] determine the lowest energy conformer to be the Gg' form. The microwave structural parameters eliminate the possibility of an OH--F hydrogen bond as the source of the stability of the Gg' conformer. Alternative explanations for this stability include a bond-dipole bond-dipole attraction between the OH and CF bonds [4,5], the "gauche" effect [6,7], and a three-center exchange interaction [8].

Matrix-isolation experiments [8-12] have shown that Gg' 2-fluoroethanol interconverts to the Tt conformer when the hydride stretching mode is irradiated by infrared light. The details of conformational isomerization at the state-specific level are still unknown despite the large effort devoted to investigating conformational isomerization in rare-gas matrices [13]. Moreover, the relationship between the matrix and the isolated molecule results is not clear because torsional (i.e.

isomerization mode) frequencies change dramatically in a matrix.

In the gas phase, excitation of the asymmetric C-H stretch of 2-fluoroethanol [14] does not show conclusive evidence for coupling to other conformers. Evidence for conformation coupling in the gas phase is difficult to obtain since the geometries and thus the rotational constants of the conformers can differ dramatically. Accordingly, interactions between conformers will only be resonant over a small range of rotational states and are likely to appear as isolated perturbations in the spectrum. By using microwave/radiofrequency-infrared multiple-resonance spectroscopy to measure the rotational spectrum of the dark state, the rotational constants can be determined and the structure of the dark state inferred.

Experimental

The molecular-beam apparatus has been described previously [15-18]. The molecular beam is a skimmed, continuous expansion from a 60 μm nozzle of ~ 100 kPa of He flowed over liquid 2-fluoroethanol. Recent reports of the toxicity of the related compound 1,2-difluoroethane suggest that 2-fluoroethanol may also have high toxicity [19].

After the skimmer the molecular beam enters a 56 cm long quadrupole state-focussing assembly. Approximately 25 cm from the end of the quadrupole rods the molecular beam impinges on a liquid-He-cooled (1.7 K) semiconductor bolometer [20]. The bolometer signal is largely due to the changing beam flux induced by the state focussing assembly, synchronous with the photon

absorption. This apparatus differs from the traditional optothermal method [20], which measures the increase in internal energy of the molecules in the molecular beam upon infrared excitation.

Infrared radiation is provided by a microwave-sideband CO₂ laser. Approximately 6 W of power from a Lamb-dip stabilized [21] CO₂ laser and 20 W of microwave power (6 to 18 GHz) from a synthesizer-driven traveling wave tube amplifier are mixed in a stripline modulator designed by Cheo [22], producing approximately 1-2 mW of tunable infrared radiation in each of the sidebands. The modulator output beam is sent into a 2 cm plane-parallel multipass cell located between the nozzle and skimmer, making approximately 15 passes through the molecular beam. The non-orthogonal crossings of the laser and molecular beams cause an absolute frequency shift of about 8 MHz. The uncertainty in the exact shift is on the order of 2 MHz and limits the absolute accuracy of the reported frequencies. The ν_{14} C-O stretch spectrum was recorded using the R(36) - R(42) lines of the 9 μm band of the CO₂ laser.

Microwave radiation from microwave synthesizers or klystrons is coupled into the laser excitation region using either an X-band (> 7.9 GHz) or K-band (> 14.1 GHz) waveguide. The waveguide terminates immediately beneath the laser multipass cell. Radiofrequency radiation (10 MHz to 9 GHz) is coupled into the molecular beam using a 2 cm long antenna placed directly above the multipass cell. The radiofrequency, microwave, and

laser fields all spatially overlap.

Results

a) The Single-Photon Infrared Spectrum

The infrared spectrum of the ν_{14} C-O stretch vibration has been assigned, aided by ground-state microwave-infrared double-resonance and precise ground-state combination differences. The nomenclature of the ν_{14} normal mode as a C-O stretch follows that of Perttilä et al. [8]. This vibration contains a nearly equal contribution from the C-F stretch internal coordinate motion, as well as lesser contributions from other motions. An a,b, and c-type hybrid band is observed, which is possible for a molecule with no plane of symmetry. The observed transitions, listed in Table I, were fit to the A-reduction of the Watson asymmetric top Hamiltonian [23] in the I' representation using a computer program written by Maki [24]. The ground-state constants were constrained in the fit to the values determined by an analysis of the microwave data of Buckton and Azrak [4], supplemented with our measured value of the $4_{31} \leftarrow 5_{23}$ transition at 3366.98 MHz. The ground state constants are given in Table II.

In the infrared analysis, eight constants were determined in a fit of 52 transition, accessing 35 different upper states including $K=0$ to 3, and $J=0$ to 9. The constants for the ν_{14} band are presented in Table II. Omitted from the fit are the transitions which terminate on the perturbed 4_{13} upper state. A section of the spectrum showing this perturbation for the $4_{13} \leftarrow 4_{04}$ transition is presented in Figure 1. The two transitions

shown are approximately equally spaced about the position predicted from the fit. The difference in the intensities of the components is most likely a result of the different state-focussing characteristics of the two upper states. The total splitting between the two transitions is 43.34(15) MHz. No evidence of the perturbation is found in adjacent J or K_a states.

The standard deviation of the infrared fit of the ν_{14} band is 0.64 MHz, which is approximately a factor of two larger than our typical experimental uncertainty of ~ 0.25 MHz. We note that the infrared ground-state combination differences agree with the microwave predicted values to 0.11 MHz, suggesting that the infrared precision is actually better than 0.1 MHz. The poor quality of the fit of the ν_{14} band might be the result of additional very weak perturbation(s) affecting the energy-level positions of the rotational levels of the ν_{14} state.

b) Rotational Spectroscopy of the Weak Perturbing State

The rotational quantum numbers and rotational constants of the perturbing state can be determined by performing microwave measurements within the perturbing state. Rotational transitions within the dark state are observed by infrared pumping one of the perturbed transitions and then scanning the microwave frequency. The perturbed states are mixtures of the ν_{14} fundamental and the dark state. The ν_{14} fundamental carries all of the infrared transition intensity from the ground state and is called the "bright" state. The perturbing state (i.e. "dark" state) is only observed when it interacts with the bright state since it has

negligible transition intensity from the ground state. In these experiments, the weak perturbation is used as a point-of-entry into the dark-state rotational manifold. All that is initially known about the rotational identity of the perturbing state is that $J = 4$. Note that symmetry does not place any constraint on the K_a or K_c quantum numbers.

Assigning the perturbing-state rotational spectrum allows the nature of the bright-state dark-state coupling mechanism (anharmonic, Coriolis, etc.) to be determined. The initial position of the bright state (E_{bright}) is known because an accurate prediction for the unperturbed position of the 4_{13} state in the ν_{14} fundamental is available from the fit of the unperturbed lines. Also, experimental values exist for the energy positions of the states after diagonalization (E_1 and E_2). The interaction matrix can be written as:

$$\begin{bmatrix} E_1 & 0 \\ 0 & E_2 \end{bmatrix} = \begin{bmatrix} E_{\text{bright}} & W \\ W & E_{\text{dark}} \end{bmatrix} \quad (1)$$

With trace conservation, $E_1 + E_2 = E_{\text{bright}} + E_{\text{dark}}$, there is enough data in the frequency information to determine both the coupling matrix element, W , and the unperturbed position of the dark state, E_{dark} . Intensity information, which is not reliable in these state-focussing measurements, is not necessary. From the frequencies of the perturbed transitions we determine that the unperturbed dark state lies 3.35(10) MHz above the unperturbed bright state (i.e. $E_{\text{dark}} - E_{\text{bright}}$). The interaction matrix element between these states is $W = 21.60(8)$ MHz.

Rotational transitions within the dark state are allowed by the rotational dipole moment of the dark state. If we express the wave function for the two interacting states as:

$$\phi_+ = \alpha |b, 4_{13}\rangle + \beta |d, 4_{31}\rangle \quad (2)$$

$$\phi_- = \beta |b, 4_{13}\rangle - \alpha |d, 4_{31}\rangle \quad (3)$$

where $|b, 4_{13}\rangle$ is the wave function for the 4_{13} bright state and $|d, 4_{31}\rangle$ is the wave function for the dark state, then the infrared intensity is proportional to $|\alpha|^2 \mu_{ir}^2$ for ϕ_+ and $|\beta|^2 \mu_{ir}^2$ for ϕ_- , where μ_{ir} is the infrared transition moment between the ground-state level and the hypothetical unperturbed 4_{13} state. Here, we have used the results of the multiple resonance measurements presented below to label the perturbing state as the 4_{31} dark state.

For rotational transitions from the perturbed states to the dark state the intensity is proportional to $|\beta|^2 \mu_{mw}^2$ for transitions originating from the ϕ_+ state and to $|\alpha|^2 \mu_{mw}^2$ for transitions originating from the ϕ_- state, where μ_{mw} is the microwave transition moment from a hypothetical unperturbed 4_{31} dark state to another dark state. In the case of the perturbation considered here, the eigenvectors from diagonalization of the Hamiltonian matrix of equation 1 gives $\alpha = 0.68$ and $\beta = 0.73$, so that both the infrared and microwave transitions are permitted with reasonable signal strength. In summary, the coefficient of $|b, 4_{13}\rangle$ permits infrared transitions to the dark state. The coefficient of $|d, 4_{31}\rangle$ determines the intensity of the rotational transitions within the dark

vibrational state.

An example of a double-resonance measurement within the dark state is shown in Fig. 2A. Here, the infrared laser is tuned to one of the perturbed transitions and the change in the signal strength is monitored as the microwave frequency is scanned. To determine whether the microwave transition terminates on a higher or lower energy state, rotational transitions from both components of the perturbation are measured. The number of possible double-resonance transitions is limited by the rotational selection rules. To reach additional states triple-resonance measurements were performed. In Fig. 2B a triple-resonance spectrum is shown. A radiofrequency transition across the asymmetry doublet at $J = 4$ permits microwave access to the other asymmetry doublet component at $J = 5$.

An energy-level diagram for the dark state showing the perturbation between the dark and bright state is presented in Fig. 3. Most of the transitions shown in figure 3 are within the $K_a = 3$ stack of the dark state. Here, the K_a assignment is made from the magnitudes of the asymmetry splittings at $J=4$ and $J=5$. The assignment of K_c is made from the ordering within the asymmetry splittings. As assigned, the splittings followed expected patterns. The ratio of the observed $J=5$ to $J=4$ asymmetry splittings is 4.05, where the predicted ratio in the limit of small asymmetry is [25] $(5+K_a)/(5-K_a)$, giving 1.5, 2.3, 4.0, 9.0, for $K_a = 1, 2, 3, \text{ and } 4$, respectively.

Discussion

a) Vibrational Assignment of the Perturbing State

From the rotational assignment of the perturbing level and the rotational constants of the dark state, a vibrational assignment can be proposed. First, we consider the possibility that the dark state arises from a different conformer of the molecule. In Table III the rotational constants for the five energetically distinct conformers are given. These constants are calculated using the structural parameters of the Gg' ground-state conformer determined from the previous microwave study [4]. The constants for the other conformers are calculated by rotating the two internal rotors (the O-H and -CH₂F rotors) in 120° increments, but making no other structural changes. The relative energies for the conformers, calculated by ab initio methods [26], are also listed in Table III.

Within the accuracy of the ab initio calculations all the conformers may be energetically accessible at 1086 cm⁻¹ above the ground state. The measured A rotational constants show that the dark state does not arise from either the Tt or Tg conformer, the two conformers closest in energy to the Gg' ground state. The rotational constants do not allow us to eliminate the Gt or Gg conformers as possible perturbers. The higher energies of the Gg and Gt conformers as determined by the ab initio calculations, however, suggest that these conformers are unlikely to be responsible for the perturbation. Furthermore, using the ab initio conformer energies and harmonic vibrational frequencies we predict that only one vibrational state from the Gg and Gt

conformers lies within a 50 cm^{-1} interval around 1086 cm^{-1} , compared to 7 states for the Gg' conformer. Thus, only the more probable case of a coupling to one of the Gg' vibrations is considered further.

In Table IV and V appears a list of vibrational overtone and combination bands occurring in the region of the dark state origin at 1086.14763(31) cm^{-1} . The frequencies of the low frequency modes are taken from infrared measurements [8,27], except for ν_{21} which is obtained from relative intensity measurements in the microwave spectrum [4]. Harmonic frequencies are used for the vibrational frequencies. For ν_{21} we have corrected for anharmonic shifts by using the experimentally determined anharmonicity of the C-C torsion in the related 1,2-difluoroethane molecule in which the torsional frequency is similar to that found in 2-fluoroethanol.

Of the states listed in Table IV, the most likely assignment of the perturber is to the state containing four quanta in the C-C torsion (ν_{21}) and 1 quantum of the CCO bending vibration at 516 cm^{-1} (ν_{18}). The dark-state rotational constants are also in accord with expected constants based on the rotational constant of the ν_{21} fundamental, known from hot-band microwave spectra [4]. In Table IV, the rotational constants of possible perturbers are given, making the assumption that all of the change in the rotational constants is dominated by the number of quanta in the lowest frequency mode, the C-C torsion. We also assume that the rotational constant change is linear in the

number of C-C torsional quanta. A near linear behavior is observed for the C-C torsion in 1,2-difluoroethane [29].

One complication in the dynamics of 2-fluoroethanol that has been neglected, is the presence of enantiomers for all but the Tt conformer. Conversion between the enantiomeric forms occurs through a complicated internal rotation pathway for 2-fluoroethanol. For example, the most stable Gg' interconverts through a rotation of both the -OH and -CH₂F rotors to the isoenergetic G'g conformer. Because of the heavy mass of fluorine, the tunneling probability between enantiomers will be small. This tunneling motion is totally quenched in the ground state, as evidenced by the observation of c-type rotational transitions. As energy is put into the C-C torsion, a coordinate leading to interconversion, the tunneling motion will become allowed. The lack of any doubling of the rotational levels and the measurement of a c-type rotational transition in the dark state indicates that the dark state tunneling rate remains negligible, even with $\sim 560 \text{ cm}^{-1}$ of energy in the large amplitude motion.

Additional spectroscopic and theoretical work is required to unambiguously confirm the assignment of the dark state. In particular, we have treated the C-C torsion and the C-O torsion as separate coordinates in the analysis. In fact, these two coordinates are intimately connected, producing a large amplitude potential surface parameterized by the two torsional angles. Since the dark state undoubtedly has a large amount of energy in

the rotor motions, the exact position of the background states, and the calculation of the rotational constants of these states requires treatment of the surface as a whole. Some effort has been made in this direction [30,31], but not at a level which allows comparison with experiment.

b) Mechanism of the $\Delta K_a = 2$ Interaction

In this section we consider the origin of the weak coupling between the 4_{13} state of the ν_{14} fundamental and the 4_{31} state of the perturbing vibration. The high-order $\Delta K_a=2$ rovibrational interaction couples rotational states having both K_a and K_c odd, corresponding to B_g symmetry within the Four Group, $V(a,b,c)$, used to classify the wavefunctions of an asymmetrical rotor [32]. The interaction is essentially anharmonic in character since it couples states of the same Four-Group symmetry. Below we show that this coupling is best understood as a folding in of the $\Delta K_a = 0$ anharmonic interaction through the nonorthogonality of the rotational wavefunctions of the two vibrational states. As an aside, we note that the 4_{13} bright state is apparently uncoupled from the nearby 4_{32} dark state, indicating that higher-order $\Delta K_a=2$ a-type Coriolis interactions, driven by molecular asymmetry, or high-order $\Delta K_a=2$ b or c-type Coriolis interactions, allowed by inertial axis rotation terms, are negligible at these J values.

The observed $\Delta K_a = 2$ matrix element between ν_{14} and the probable dark state $\nu_{18}+4\nu_{21}$ can be used to estimate the $J=0$ anharmonic interaction between these states. We consider the approximate Hamiltonian,

$$H = H_{\text{vib}} + H_{\text{anh}} + H_{\text{rot}} , \quad (4)$$

where H_{vib} gives the normal-mode frequencies with diagonal anharmonic corrections, H_{anh} gives the off-diagonal anharmonicities between the normal modes and their combination vibrations, and H_{rot} is the asymmetric-top rotational Hamiltonian,

$$H_{\text{rot}} = AJ_a^2 + BJ_b^2 + CJ_c^2, \quad (5)$$

where A, B, and C are the rotational constants parameterized in terms of the vibrational coordinates. Here, we have neglected Coriolis interactions and rotational angular-momentum cross-product terms ($J_i J_j$) in the molecular Hamiltonian, which are expected to be small compared to the anharmonic interactions for low J values. We choose as a vibrational basis, eigenfunctions of $H_{\text{vib}} + H_{\text{anh}}$,

$$\phi_b = \cos\alpha |b\rangle - \sin\alpha |d\rangle \quad (6)$$

$$\phi_d = \sin\alpha |b\rangle + \cos\alpha |d\rangle \quad (7)$$

where $|b\rangle$ and $|d\rangle$ are the eigenfunctions of H_{vib} for ν_{14} and $\nu_{18} + 4\nu_{21}$ in the absence of any anharmonic coupling between the states. Note that using this basis set states which are observed to be coupled by the $\Delta K_a = 2$ matrix element are already mixed by the stronger $\Delta K_a = 0$ anharmonic interaction.

The measured interaction matrix element between the 4_{13} state of ϕ_b and the 4_{31} state of ϕ_d is,

$$\langle \phi_b, 4_{13}(b) | H_{\text{rot}} | \phi_d, 4_{31}(d) \rangle \quad (8)$$

where $|4_{13}(b)\rangle$ and $|4_{31}(d)\rangle$ are eigenfunctions of the rotational Hamiltonians,

$$H_{\text{rot},b} \equiv$$

$$\langle \phi_b | H_{\text{rot}} | \phi_b \rangle = \langle \phi_b | A | \phi_b \rangle J_a^2 + \langle \phi_b | B | \phi_b \rangle J_b^2 + \langle \phi_b | C | \phi_b \rangle J_c^2 \quad (9)$$

and

$$H_{\text{rot},d} \equiv$$

$$\langle \phi_d | H_{\text{rot}} | \phi_d \rangle = \langle \phi_d | A | \phi_d \rangle J_a^2 + \langle \phi_d | B | \phi_d \rangle J_b^2 + \langle \phi_d | C | \phi_d \rangle J_c^2 \quad (10)$$

for the anharmonically mixed states.

The $|4_{13}(b)\rangle$ and $|4_{31}(d)\rangle$ wavefunctions are not orthogonal functions. We reexpress these functions in terms of the Wang symmetrized symmetric-rotor functions,

$$|JK\pm\rangle = [|JK\rangle \pm |J-K\rangle] / 2^{1/2}, \quad (11)$$

giving,

$$|4_{13}(b)\rangle = \sin\alpha_1 |43+\rangle + \cos\alpha_1 |41+\rangle \quad (12)$$

$$|4_{31}(d)\rangle = \cos\alpha_2 |43+\rangle - \sin\alpha_2 |41+\rangle, \quad (13)$$

where $\sin\alpha_1 = -0.04137$, $\sin\alpha_2 = -0.03463$, $\cos\alpha_1 = 0.99914$, and $\cos\alpha_2 = 0.99940$ are known from the diagonalization of the Watson rotational Hamiltonians using the constants of Table II.

We can use the above rotational wavefunctions to express $\langle \phi_b, 4_{13}(b) | H_{\text{rot}} | \phi_d, 4_{31}(d) \rangle$ in terms of the known matrix elements of H_{rot} in the $|d\rangle$, $|b\rangle$, and $|JK\pm\rangle$ basis functions. In this representation the experimental coupling matrix element scales as $|\sin\alpha\cos\alpha| \sim W_{bd} / (E_b - E_d)$, where W_{bd} is the $J=0$ anharmonic matrix element, and E_b and E_d are the uncoupled bright and dark state origins. When we express $\langle \phi_b, 4_{13}(b) | H_{\text{rot}} | \phi_d, 4_{31}(d) \rangle$ in terms of known matrix elements we find that the coupling matrix element has contributions from two terms. One term depends on the differences between the matrix elements of the rotational constants for the bright and dark states, $(\langle b | H_{\text{rot}} | b \rangle - \langle d | H_{\text{rot}} | d \rangle)$,

while the other term depends on the direct coupling of the dark and bright states through rotation, $\langle d|H_{rot}|b\rangle$. The latter term requires an interchange of 6 vibrational quanta through H_{rot} and is expected to be smaller than $(\langle b|H_{rot}|b\rangle - \langle d|H_{rot}|d\rangle)$, which only requires that the rotational constants for the bright and dark state be different. Nonresonant $\langle d|H_{rot}|b\rangle$ terms contribute to the centrifugal distortion constants of the bright state. The matrix element contributions from $\langle d|H_{rot}|b\rangle$ must be small based on our observation that the ground and bright state distortion constants are nearly the same.

Neglecting terms of the type $\langle d|H_{rot}|b\rangle$ we find that

$$\begin{aligned} \langle \phi_b, 4_{13}(b) | H_{rot} | \phi_d, 4_{31}(d) \rangle = & \\ \cos\alpha \sin\alpha \{ \cos\alpha_2 \sin\alpha_1 [\langle b, 43+ | H_{rot} | b, 43+ \rangle - \langle d, 43+ | H_{rot} | d, 43+ \rangle] & \\ - \cos\alpha_1 \sin\alpha_2 [\langle b, 41+ | H_{rot} | b, 41+ \rangle - \langle d, 41+ | H_{rot} | d, 41+ \rangle] & \\ + (\cos\alpha_1 \cos\alpha_2 - \sin\alpha_1 \sin\alpha_2) \times & \\ [\langle b, 43+ | H_{rot} | b, 41+ \rangle - \langle d, 43+ | H_{rot} | d, 41+ \rangle] \} . & \quad (14) \end{aligned}$$

If the anharmonic interaction is small compared to the energy separation between the two states we can further assume that the measured dark and bright state rotational constants are not strongly mixed by the anharmonic interaction. Terms such as $\langle b|A|b\rangle$ and $\langle d|A|d\rangle$ can be approximated by the experimental values of $\langle \phi_b|A|\phi_b\rangle$ and $\langle \phi_d|A|\phi_b\rangle$ from Table II. From the above expression we determine a value of 0.0403 for $|\cos\alpha \sin\alpha|$, corresponding to a value of ~ 3.5 GHz for the $J=0$ anharmonic coupling between the states. Since the noninteracting bright and dark state origins are separated by nearly 3 cm^{-1} the 3.5 GHz

anharmonic term has a negligible effect on the energy level positions, shifting them approximately 140 MHz for $J=0$.

The coupling term invoked here is similar to the vibrationally induced inertial axis rotation (VIRAS) mechanism of Li, Ezra, and Philips [33], in that the rotational wave functions for the bright and dark state are not orthogonal. The approaches differ, however, in the mechanism which generates this nonorthogonality. Li et al. [33] invoke a vibrationally induced inertial axis rotation to give the nonorthogonality. We only require that the dark and bright state rotational constants be different. The nonorthogonality of the rotational wave functions for different vibrational states allows an essentially $\Delta K_v=0$ anharmonic matrix element to couple states of different K . VIRAS will give both ΔK_v -odd and ΔK_v -even couplings whereas the present mechanism will only give ΔK_v -even couplings.

c) Implications for Intramolecular Vibrational Energy Redistribution at Higher Energies.

At higher energies, such as the region of the hydride stretches, the density of bath states can be sufficiently large that isolated perturbations occur frequently, as seen in the case of the acetylenic C-H stretch fundamental of CF_3CCH [34]. These weak, near-resonant interactions couple additional states in the spectrum without adding much total coupling strength. The density of coupled states increases as a function of the total angular momentum, J , but the width over which the perturbations are observed, which is a measure the time scale of energy

localization in the bright state, remains unchanged.

To explain the interaction in 2-fluoroethanol we have invoked a rotationally-induced anharmonic mixing due to the non-orthogonality of the rotational wavefunctions in states with different rotational constants. This mechanism only mixes states for which ΔK_a and ΔK_c are even. Here, limited K-mixing occurs even though all the vibrational coupling is strictly anharmonic. As a result of the K mixing, the density of observed states in a highly perturbed spectrum will grow as $(2J+1)/4$ for a given value of K_a for the bright state. Coriolis and axis-rotation terms allow coupling between all four Wang blocks, opening up the full $(2J+1)$ set of rovibrational states. In general, an asymmetric-top molecule in a region of high state density is expected to show the full $(2J+1)$ state-density increase. [35,36]

The mechanism presented here enables the calculation of high-order rovibrational coupling matrix elements in asymmetric tops when the anharmonic matrix element between the vibrational states, and the rotational constants of the states are known. Both of these values can be estimated from third and fourth-order anharmonic constants determined from ab initio calculations. Gaw et al. [37] and Green et al. [38] have shown that accurate rotational constants for highly excited vibrational states of polyatomic molecules can be determined from an ab initio calculation. Furthermore, it has been demonstrated that the high-order (in vibrational quantum interchange) anharmonic and Coriolis coupling strengths can be obtained through Van Vleck

perturbation formulas using the third-order ab initio anharmonic terms.[39] Together, these results suggest that an ab initio predictive theory of IVR could be developed.

Lastly, we note that the present matrix element is on the order of the average coupling matrix elements observed in highly perturbed spectra in the region of the hydride stretch. For example, the measured average matrix elements for the C-H stretches of CF_3CCH [34], $\text{HCCCH}_2\text{NH}_2$ [36], HCCCH_2OH [40], and 2-fluoroethanol [14] are all less than 300 MHz. These weak matrix elements suggest that the dilution of the full anharmonic matrix element through a high-order rotational effect, such as observed here where a 3.5 GHz anharmonic matrix element appears as a 21.6 MHz coupling, is a common occurrence in spectra at higher state density.

Conclusions

We have shown for 2-fluoroethanol that microwave measurements in the excited vibrational state can overcome some of the limitations of a single-photon absorption spectrum. The microwave measurements yield the type of coupling between the dark and bright state and the rotational constants of the dark state. The dark state is assigned to a torsionally excited level of a lower frequency normal mode of the most stable conformer. The coupling has a $\Delta K_a = 2$, $\Delta K_c = 2$ selection rule and arises from the non-orthogonality of the rotational wavefunctions of the bright and dark states, which occurs in an asymmetrical top when the two interacting vibrational states have different rotational

constants. The rotationally-induced anharmonic coupling has a matrix element of 21.6 MHz, compared to the 3.5 GHz $\Delta K_a = 0$ anharmonic term. Such weak $\Delta K_a \neq 0$ or $\Delta K_c \neq 0$ coupling are expected to be a general feature of vibrational spectra in higher vibrational density of states regimes.

References

1. K.F. Freed and A. Nitzan, *J. Chem. Phys.* **73**, 4765 (1980).
2. T.A. Brody, J. Flores, J.B. French, P.A. Mello, A. Pandey, and S.S.M. Wong, *Rev. Mod. Phys.* **53**, 385 (1981).
3. W.D. Lawrance and A.E.W. Knight, *J. Phys. Chem.* **89**, 917 (1985).
4. K.S. Buckton and R.G. Azrak, *J. Chem. Phys.* **52**, 5652 (1970).
5. R.G. Axrak and E.B. Wilson, *J. Chem. Phys.* **52**, 5299 (1970).
6. J. Huang and K. Hedberg, *J. Am. Chem. Soc.* **111**, 6909 (1989).
7. S. Wolfe, *Acc. Chem. Res.* **5**, 102 (1972).
8. M. Perttilä, J. Murto, A. Kivinen, and K. Turunen, *Spectchim. Acta* **34A**, 9 (1978).
9. J. Pourcin, G. Davidovics, H. Bodot, L. Abouaf-Marguin, and B. Gauthier-Roy, *Chem. Phys. Lett.* **74**, 147 (1980).
10. G. Davidovics, J. Pourcin, M. Monnier, P. Verlaque, H. Bodot, L. Abouaf-Marguin and B. Gauthier-Roy, *J. Mol. Struct.* **116**, 39 (1984).
11. J. Pourcin, M. Monnier, P. Verlaque, G. Davidovics, R. Lauricella, C. Colonna, and H. Bodot, *J. Mol. Spectrosc.* **109**, 186 (1985).
12. J.S. Shirk and C.L. Marquardt, *J. Chem. Phys.* **92**, 7234 (1990).
13. For a review see H. Frei and G.C. Pimentel, *Ann. Rev. Phys. Chem.* **36**, 491 (1985).
14. C.L. Brummel, S.W. Mork, and L.A. Philips, *J. Chem. Phys.* **95**, 7041 (1991).

30. A. Allouche and J. Pourcin, *J. Mol. Struct.* **192**, 29 (1989).
31. B.D. El-Issa and R.N. Budeir, *J. Mol. Struct.* **232**, 249 (1991).
32. G.W. King, R.M. Hainer, and P.C. Cross, *J. Chem. Phys.* **11**, 27 (1943).
33. H. Li, G.S. Ezra, and L.A. Philips, *J. Chem. Phys.* **97**, 5956 (1992).
34. B.H. Pate, K.K. Lehmann, and G. Scoles, *J. Chem. Phys.* **95**, 3891 (1991).
35. J. Go, G.A. Bethardy, D.S. Perry, *J. Phys. Chem.* **94**, 6153 (1990).
36. A.M. Andrews, G.T. Fraser, and B.H. Pate, "High Resolution Spectroscopy, Summaries of papers presented at the High Resolution Spectroscopy Topical Meeting", 1993 Technical Digest Series, (Optical Society of America, Washington, D.C., 1993) Vol 1. p. 44, and unpublished results.
37. J.F. Gaw, A. Willetts, W.H. Green, and N.C. Handy, Advances on Molecular Vibrations and Collision Dynamics, edited by J.M. Bowman (JAI Press, Greenwich, CT, 1990).
38. W.H. Green, D. Jayatilaka, A. Willetts, R.D. Amos, and N.C. Handy, *J. Chem. Phys.* **93**, 4965 (1990).
39. K.K. Lehmann, *J. Chem. Phys.* **96**, 1636 (1992).
40. G.T. Fraser and B.H. Pate, unpublished.

Table I. Observed infrared transition frequencies for the ν_{14} C-O stretching fundamental of 2-fluoroethanol (in cm^{-1}).

ν	J''	K _a ''	K _c ''	J'	K _a '	K _c '	ν	J''	K _a ''	K _c ''	J'	K _a '	K _c '
1086.294799	8	1	8	9	0	9	1088.678284	3	2	2	4	1	3
1086.439954	7	0	7	8	1	8	1088.686931	1	0	1	1	1	0
1086.498306	5	3	2	5	4	1	1089.375994	2	0	2	1	1	1
1086.498841	6	3	3	6	4	2	1089.429539 ^a	4	1	3	3	2	2
1086.499511	4	3	1	4	4	0	1089.430988 ^a	4	1	3	3	2	2
1086.530618	3	1	3	4	2	2	1089.441932	1	1	0	1	0	1
1086.627311	7	1	7	8	0	8	1089.471023	2	1	1	2	0	2
1087.193514	6	2	5	6	3	4	1089.517994	3	1	2	3	0	3
1087.213726	5	2	4	5	3	3	1089.585792 ^a	4	1	3	4	0	4
1087.226741	4	2	3	4	3	2	1089.587234 ^a	4	1	3	4	0	4
1087.242919	3	2	1	3	3	0	1089.680414	5	1	4	5	0	5
1087.245384	4	0	4	5	1	5	1089.725101	2	0	2	1	0	1
1087.251558	4	2	2	4	3	1	1089.727806	3	0	3	2	1	2
1087.269655	5	2	3	5	3	2	1089.744553	1	1	1	0	0	0
1087.293240	1	1	1	2	2	0	1089.744553	1	1	1	0	0	0
1087.299824	6	2	4	6	3	3	1090.332468	3	1	3	2	0	2
1087.318846	5	1	5	6	0	6	1090.442095	5	0	5	4	1	4
1087.322021	1	1	0	2	2	0	1090.455693	6	2	5	6	1	6
1087.323804	1	1	0	2	2	1	1090.559852	7	2	6	7	1	7
1087.448227	6	2	5	7	1	6	1090.607200	4	1	4	3	0	3
1087.454562	9	2	7	9	3	6	1090.632633	7	1	6	6	2	5
1088.385749	0	0	0	1	1	1	1090.635105	5	1	5	4	1	4
1088.397670	2	1	2	3	0	3	1090.647457	8	3	5	8	2	6
1088.426103	5	0	5	5	1	4	1090.716736	7	3	4	7	2	5
1088.430739	1	1	1	2	1	2	1090.732580	5	2	3	4	2	2
1088.527395	4	0	4	4	1	3	1091.380193	4	2	3	3	1	2
1088.602237	3	0	3	3	1	2	1091.399229	7	1	7	6	0	6
1088.654290	2	0	2	2	1	1	1091.479121	8	0	8	7	1	7
							1091.582165	4	2	2	3	1	3

^a 4_{13} upper state perturbed, see text.

Table II. Spectroscopic constants (in MHz) for the ground state, ν_{14} C-O stretching fundamental vibration, and perturbing state for 2-fluoroethanol.

	ground state ^a	ν_{14} C-O stretch	Perturbing State
ν_0 (cm ⁻¹)	---	1089.0662576(68) ^b	1086.14763(31)
A	15875.248(42)	15809.82(12)	16466.28(67)
B	5409.156(17)	5387.899(31)	5247.23(99)
C	4525.814(18)	4525.018(29)	4455.29(64)
Δ_J	0.00887(33)	0.00877(19)	0.0347(40)
Δ_{JK}	-0.0428(25)	-0.0388(22)	-0.0428 ^c
Δ_K	0.1064(39)	0.067(14)	0.1064 ^c
δ_J	0.00241(12)	0.00288(19)	0.00241 ^c
δ_K	0.0186(48)	0.0186 ^c	0.70(20)
σ^d	0.13	0.64	0.20

^a Constants determined from the data of reference [4] plus our measurement of the $4_{31} - 5_{23}$ transition at 3366.98 MHz.

^b Uncertainties are one standard error in units of the last significant digit shown.

^c Indeterminate, constrained to the ground-state value.

^d Standard deviation of the fit.

Table III. Comparison of the dark state rotational constants with the estimated rotational constants for five conformers of 2-fluoroethanol (in MHz).

	Dark State	Gg'	Gg	Gt	Tg	Tt
A	16466	15982	16125	16785	30983	32558
B	5247	5443	5294	5171	3898	3830
C	4455	4538	4547	4411	3650	3581
Energy ^a (cm ⁻¹)		0	1388	1044	765	507

a) Relative energy of the conformers of 2-fluoroethanol calculated at the MP3/4-31G level: Ref. [26].

Table IV. Estimated spectroscopic constants for possible perturbing states nearly resonant with the C-O stretching vibration.

State Assignment	ν_0 (cm ⁻¹) ^a	ΔA (MHz) ^b	ΔB (MHz)	ΔC (MHz)
Dark*	1086	591	-162	-71
$\nu_{19} + 5\nu_{21}$	1044	702	-164	-87
$\nu_{18} + 2\nu_{20}$	1084	---	---	---
$\nu_{18} + 4\nu_{21}$	1089	562	-131	-70
$\nu_{18} + \nu_{20} + 2\nu_{21}$	1099	281	-66	-35
$2\nu_{19} + \nu_{20} + \nu_{21}$	1122	140	-33	-17
$2\nu_{19} + 3\nu_{21}$	1125	421	-98	-52
$4\nu_{20}$	1136	---	---	---

* Experimental values for the dark state from Table II.

^a Harmonic estimates of the band origins based on gas phase absorption frequencies. The ν_{21} vibrational ladder has been corrected for anharmonicity.

^b Estimates of the change in rotational constants due to excitation of ν_{21} (see text).

Table V. Calculated spectroscopic constants for different vibrational levels of the torsion, ν_{21} .

quanta of ν_{21}	A (MHz)	B (MHz)	C (MHz)
0	15875	5409	4525
1	16015	5376	4508
2	16156	5343	4490
3	16296	5311	4473
4	16437	5278	4455
5	16577	5245	4438

Figure Captions

Figure 1. Spectral window of the ν_{14} C-O stretching fundamental band of 2-fluoroethanol showing the $4_{13} \leftarrow 4_{04}$ transition being split into a doublet by a perturbation with a $J=4$ background state. The spectrum was recorded with the CO_2 laser stabilized on the R(38) transition of the 9 μm band of CO_2 . The microwave frequency synthesizer was stepped from 17500 to 17600 MHz in 500 kHz steps using a time constant of 125 ms.

Microwave/radiofrequency-infrared multiple resonance spectroscopy identifies the rotational quantum numbers of the perturbing state as 4_{31} . The predicted position of the unperturbed 4_{13} bright state is shown by the arrow.

Figure 2. A. Microwave-infrared double-resonance spectrum obtained by monitoring the signal strength of the lower frequency component of the perturbed $4_{13} \leftarrow 4_{04}$ infrared transition of the ν_{14} C-O stretch as a function of microwave frequency. The microwave transition terminates on the unperturbed 5_{32} level of the dark state and originates on the lower energy state arising from the perturbation between the 4_{13} bright state and the 4_{31} dark state.

B. Microwave-radiofrequency-infrared triple-resonance spectrum showing the $5_{33} \leftarrow 4_{32}$ dark-state transition. The spectrum was obtained by monitoring the signal strength of the lower frequency component of the perturbed $4_{13} \leftarrow 4_{04}$ infrared transition. A cw radiofrequency oscillator was fixed at 14.98 MHz, corresponding to the transition frequency between the lower energy component of the perturbed 4_{13} state and the 4_{32} dark state. The microwave source was then tuned from 48620 to 48627 MHz to observe the $5_{33} \leftarrow 4_{32}$ dark state line.

Figure 3. Energy-level diagram showing the perturbation between the 4_{13} light state of the ν_{14} C-O and the 4_{31} level of a background vibrational state. Also shown are the $J=5$, $K_a=3$ and $J=3$, $K_a=3$ levels of the dark state. The measured frequencies in MHz for the observed radiofrequency and microwave transitions used in constructing the energy level diagram for the dark state are also given. All transitions originating from the 4_{32} level of the dark state are triple resonance measurements. The measurement of the asymmetry splitting of the 5_{32} and 5_{33} levels of the dark state are also made using three photons.